

# **Poly(Acrylic Acid) with Disulfide Bond for the Elaboration of pH-Responsive Brush Surfaces**

Wim Van Camp<sup>1</sup>, Filip E. Du Prez<sup>1\*</sup>

*<sup>1</sup>Ghent University, Department of Organic Chemistry, Polymer Chemistry Research Group,  
Krijgslaan 281 (S4bis), 9000 Ghent, Belgium.*

Halima Alem<sup>2</sup>, Sophie Demoustier-Champagne<sup>2\*</sup>

*<sup>2</sup>Université catholique de Louvain, Unité de Physique et de Chimie des Hauts Polymères,  
Croix du Sud 1, 1348 Louvain-la-Neuve, Belgium*

Nicolas Willet<sup>3</sup>, Georgy Grancharov<sup>3</sup>, Anne-Sophie Duwez<sup>3\*</sup>

*<sup>3</sup>University of Liège, Department of Chemistry, NanoChemistry and Molecular Systems, B6a  
Sart-Tilman, 4000 Liège, Belgium.*

\* Corresponding authors:

F. E. D. P.: Tel. +32 9 2644503. Fax: +32 9 2644972. E-mail: [filip.duprez@ugent.be](mailto:filip.duprez@ugent.be)

S. D.-C.: Tel.: +32 10 472702. Fax: +32 10 451593. E-mail: [sophie.demoustier@uclouvain.be](mailto:sophie.demoustier@uclouvain.be)

A.-S. D: Tel. +32 4 3663482, Fax. +32 4 3663497. E-mail: [asduwez@ulg.ac.be](mailto:asduwez@ulg.ac.be)

## ABSTRACT

We report on a new route for the facile preparation of pH-responsive tethered brushes on metallic surfaces, starting from poly(acrylic acid) (PAA) containing a disulfide (S-S) bond (PAA-S-S-PAA). First, atom transfer radical polymerization (ATRP) of 1-ethoxyethyl acrylate (EEA) with a disulfide containing initiator was performed to obtain the poly(EEA) precursor polymer (PEEA-S-S-PEEA). Deprotection of PEEA by a heating step resulted in the desired PAA-chains without any further purification. The brushes, obtained by the 'grafting to' of PAA-S-S-PAA onto gold, were then characterized by atomic force microscopy in water at various pH values. The results evidence a large collapsing/swelling capacity.

## KEYWORDS

Poly(acrylic acid), pH-responsive surface, gold, AFM, 1-ethoxyethyl acrylate, disulfide

## INTRODUCTION

The fabrication of stimulus-responsive surfaces has attracted considerable attention in recent years because of potential applications in many fields ranging from biotechnology and biomaterials to advanced microelectronics [1]. Smart responsive polymer coatings can adapt or change surface properties (wetting, reactivity, adhesion, roughness, mechanics,...) via external stimuli. Controlled radical polymerization techniques have been widely applied for the elaboration of such materials as they allow for the precise synthesis of macromolecules with controlled molecular weight, composition and functionality [2-5]. Among the various methods reported to prepare polymer brushes on surfaces, 'grafting-from' and 'grafting-to' strategies provide a route to brushes that are covalently bound to the substrate [6, 7]. The 'grafting-from' strategy consists in a surface initiated polymerization starting from immobilized initiators. Atom transfer radical polymerization (ATRP) has been the most

widely employed technique for the formation of polymer brushes with controlled molecular weight and narrow molecular weight distribution via surface initiated polymerization [8]. The 'grafting-to' strategy refers to preformed, end-functionalized, polymers reacting with a suitable surface under appropriate conditions to form a tethered polymer brush. One of the limitations of 'grafting to' compared to 'grafting from' is the relatively low surface density obtained, due to the steric hindrance of grafted chains, which inhibits diffusion of large free polymer chains to open-surface reactive sites. On the other hand, this drawback turns into an advantage for the creation of stimuli-responsive surfaces: a moderate grafting density enables a large collapsing/swelling capacity and thus a high efficiency of the responsive behavior. In the last few years, it has been demonstrated that reversible addition fragmentation chain transfer (RAFT) polymerization is a convenient strategy for 'grafting to' approaches. As a consequence of the mechanism, polymers prepared by RAFT bear a dithioester end group, or a trithiocarbonate group in the middle of the chain, according to the type of chain transfer agent (CTA) that is used. Polymers produced by RAFT are thus highly interesting for the functionalization of metal surfaces, and in particular gold, via the 'grafting-to' approach. The usual procedures to modify gold surfaces with RAFT polymers involve the transformation of the sulfur-containing group coming from the CTA into thiols or disulfides by reaction with nucleophiles such as primary amines [9-13]. Recently, Duwez *et al.* showed that the transformation of dithioesters and trithiocarbonates into thiols or disulfides was not mandatory for the functionalization of metal surfaces, as these two species are able to chemisorb onto gold with a grafting density close to the one obtained with thiols [14-16]. However, the RAFT process shows some limitations such as the rather slow kinetics of the polymerization process and the limited complexity of architectures that can be synthesized [17, 18]. For example, the synthesis of star or brush copolymers is more easily achieved by ATRP [3, 19-21]. As this polymerization technique allows for a wider range of accessible

polymer architectures, it is expected to further expand the range of applications for smart surfaces [22, 23]. For that reason, there is a strong interest in developing new ATRP methods for the 'grafting to' approach.

Here, we report on a new and facile route to prepare gold surfaces with pH-switchable properties by tethering poly(acrylic acid) (PAA) containing a disulfide (S-S) bond (PAA-S-S-PAA) prepared by ATRP. The disulfide functionality was simply introduced by the use of a disulfide containing ATRP initiator [24, 25], while the PAA was obtained *via* the polymerization of 1-ethoxyethyl acrylate followed by a thermal deprotection step [26-28], avoiding any further purification process. Characterization of the pH-responsive behavior was done by atomic force microscopy in water.

## EXPERIMENTAL DETAILS

### Materials

1-Ethoxyethyl acrylate monomer was synthesized as described before [28]. Acrylic acid (Acros Organics, 99.5 %) was purified by distillation with phenothiazine as inhibitor. Ethyl vinyl ether (Aldrich, 99 %) was distilled before use.  $\text{Mg}_6\text{Al}_2(\text{OH})_{16}\text{CO}_3 \cdot 4\text{H}_2\text{O}$  was obtained from Kisuma Chemicals.  $\text{Cu(I)Br}$  was purified first by stirring with acetic acid, then by washing with methanol, and finally by drying in a vacuum oven at 70 °C. *N,N,N',N'',N''*-pentamethyldiethylenetriamine (PMDETA, Aldrich, 99 %) was distilled (85-86 °C/12 mmHg). Solvents were purchased from Aldrich (HPLC grade) and used without purification. All other chemicals were used as received.

Gold substrates (150 nm of Au(111) films on mica prepared from thermal evaporation of gold) were purchased from Agilent Technologies.

### Characterization

$^1\text{H}$  NMR spectra were recorded on a Bruker Avance 300 spectrometer (300 MHz) at room temperature. Gel permeation chromatography (GPC) was carried out on a Waters instrument, with refractive index (RI) detector (2410 Waters), equipped with  $10^3$  -  $10^4$  and  $10^5$  Å serial columns. Polystyrene (PS) standards were used for calibration, and  $\text{CHCl}_3$  was used as an eluent at a flow rate of  $1.5 \text{ mL min}^{-1}$ . Data were analyzed using Image Pro Plus software. Infrared spectra were obtained with a Perkin Elmer 1600 Series FTIR. Thermogravimetric analysis was done with a Thermal Sciences PL-TGA 1000 system or with a Mettler Toledo TGA/SDTA851e instrument under air or nitrogen atmosphere at a heating rate of  $10 \text{ }^\circ\text{C/min}$  from  $25 \text{ }^\circ\text{C}$ - $800 \text{ }^\circ\text{C}$ . XPS was performed on a SSIX probe (SSX 100/206) spectrometer from Fisons equipped with a monochromatic Al  $\text{K}\alpha$  X-ray source ( $h\nu = 1486.7 \text{ eV}$ ). Spectra were recorded at a take-off angle of  $35^\circ$  (angle between the plane of the sample surface and the entrance lens of the analyzer) with a pass energy of  $150 \text{ eV}$ . AFM-based force spectroscopy experiments and imaging were carried out in water (at pH 5 prepared from HCl or pH 9 prepared from NaOH). Images were obtained with a PicoSPM equipped with a fluid cell (Molecular Imaging) and controlled by Nanoscope III electronics (Digital Instruments). Force spectroscopy experiments were carried out with a PicoPlus equipped with a fluid cell (Agilent Technologies). Silicon nitride gold-coated tips (Microlevers®, Veeco) covered with decanethiols (Sigma-Aldrich) were used. The presence of the alkanethiol layer prevents the apparition of charges at the tip surface. Bare silicon nitride tips are likely to be charged in water, which can give rise to repulsion when interacting with the charged PAA. Since we evaluate the thickness of the layers through the repulsive profile induced by compression, any other contribution to this repulsion must be excluded.

**Preparation of PEEA-S-S-PEEA: ATRP of EEA with disulfide-containing initiator bis(2-hydroxyethyl)disulfide bis(2-bromopropionate).**

Bis(2-hydroxyethyl)disulfide bis(2-bromopropionate) was synthesized according to a literature procedure [24, 25]. A typical polymerization procedure is as follows (e.g. entry 1): Prior to use, EEA was passed through a small column of basic  $\text{Al}_2\text{O}_3$  to remove traces of acrylic acid. A mixture of 0.0347 mol (5.0 mL) of the monomer EEA and  $0.347 \cdot 10^{-3}$  mol (0.072 mL) of PMDETA as the ligand was added to a reaction flask and was bubbled with  $\text{N}_2$  for 1h to remove oxygen from the reaction mixture. After that,  $\text{Cu(I)Br}$  ( $0.347 \cdot 10^{-3}$  mol, 0.050 g) was added and the reaction flask was placed in an oil bath at  $50^\circ\text{C}$ . When the reaction mixture reached the desired reaction temperature, the polymerization was started by adding  $0.694 \cdot 10^{-3}$  mol (0.098 mL) of bis(2-hydroxyethyl)disulfide bis(2-bromopropionate) as the initiator. Samples were withdrawn periodically to monitor the monomer conversion (by  $^1\text{H}$  NMR) and the average molecular weight (by GPC). The reaction was terminated by cooling the reaction mixture in liquid nitrogen. The resulting polymer was dissolved in THF and the diluted reaction mixture was passed over a column of neutral  $\text{Al}_2\text{O}_3$  to remove the copper catalyst. The excess of solvent was removed and the residual monomer was removed by high vacuum.

#### **Deprotection of PEEA-S-S-PEEA to PAA-S-S-PAA.**

Deprotection of PEEA-S-S-PEEA to the corresponding PAA-S-S-PAA was done by a heating step. The PEEA-S-S-PEEA sample was spread out on a glass surface and heated in an oven at  $80^\circ\text{C}$  for 24 h [26, 27].

#### **Preparation of the brush surfaces.**

The gold substrates were cleaned by UV–ozone treatment (5 min.), immersed 20 min. in ethanol, and finally immersed in a solution of PAA-S-S-PAA in ethanol (1g/l) for 72 h. The samples were copiously rinsed with ethanol and dried with a flux of nitrogen.

## **RESULTS AND DISCUSSION**

Acrylic acid can not be polymerized directly via ATRP because of a side reaction of the acid group with the transition metal complex [29]. Therefore, the preparation of PAA-S-S-PAA was started with ATRP of the protected monomer 1-ethoxyethyl acrylate [17, 26-28, 30, 31] (EEA) (see Figure 1), by making use of a disulfide-containing initiator: bis(2-hydroxyethyl) disulfide bis(2-bromopropionate) (BHEDS(BP)<sub>2</sub>) [24, 25]. After polymerization of EEA, the PEEA-S-S-PEEA was deprotected to yield PAA-S-S-PAA by a simple heating step. In the following paragraph, the synthesis of well-defined PAA-S-S-PAA is discussed in detail.

### Figure 1

### Table 1

Table 1 gives an overview of the reaction conditions and the results of the different ATRP polymerizations that were performed. For the first experiment (entry 1, Table 1), a ratio of monomer/initiator/catalyst/ligand  $[M]_0/[In]_0/[Cu]_0/[ligand] = 100/1/0.5/0.5$  was used. To check whether the polymerization of EEA under these reaction conditions exhibits a controlled character, a kinetic study was performed (Figure 2). The first order kinetic plot shows a deviation from linearity after about 2 hours reaction time. Deviation from linearity in the first order kinetic plot is observed when the concentration of radicals in the system decreases. Often, this decrease results from the combination of radical species, which occurs when the concentration of radicals in the polymerization is too high. However, in this case, it is more likely to arise from a side reaction between the monomer and the copper catalyst. During the polymerization of EEA, it can not be avoided at relatively long reaction times that a small amount of the monomer (or the corresponding polymer) shows some deprotection, resulting in a small concentration of carboxylic acid groups in the polymerization mixture, which form an insoluble complex with the Cu(II) species [29]. As a result, the actual copper concentration and thus the concentration of radicals is lowered.

## Figure 2

## Figure 3

In addition, if the decrease of the radical concentration arises from radical termination, the GPC analysis would reveal a broadened molecular weight distribution with traces of high molecular weight species (coupling reactions) and/or traces of low molecular weight polymers (dead chains). In our case, a symmetrical GPC curve is obtained, which confirms the hypothesis of partial deprotection (see Figure 3). For entry 1 (Table 1), the polymerization stops at about 20% monomer conversion, and a number average molecular weight ( $M_n$ ) of  $3800 \text{ g.mol}^{-1}$  was reached.

The next set of ATRP reactions was performed in order to find the right reaction conditions to obtain polymers with a higher molecular weight. As the copper concentration is considered as an important polymerization parameter, the influence of the copper concentration was further examined. For entry 2 (Table 1), in which a four times higher copper concentration was used, a conversion of 68 % was reached in a shorter time. However, the molecular weight distribution, which shows a multimodal character, reveals that control over the polymerization reaction is lost under these conditions (see Figure 3, dotted line).

If the same reaction conditions are applied, but with an increase of the theoretical degree of polymerization ( $DP_{th}$ ) to 200, the reaction exhibited a controlled behavior (entry 3, Table 1 and Figure 4, ■). Although the conversion was lower, a higher  $M_n$  was reached ( $12800 \text{ g.mol}^{-1}$ ) because of the increased  $DP_{th}$ . An increase of the copper concentration (entry 4, Table 1) under these conditions resulted in a higher conversion (75 %), but just as in the case of entry 2, control over the polymerization was lost, as evidenced by the high polydispersity index (PDI) of the obtained polymer (1.67). Further increase of  $DP_{th}$  resulted in a controlled behavior of the polymerization reaction with rather low conversion (21 %).



In a next set of polymerizations, the influence of the polymerization temperature was investigated. Starting from the conditions that were applied for entry 3 (Table 1) with a ratio of  $[M]_0/[In]_0/[Cu]_0/[ligand] = 200/1/2/2$  at 50 °C, the polymerization temperature was increased to 60 °C to increase the reaction rate (entry 6, Table 1). This resulted in a higher monomer conversion (61 %) and thus in a polymer with a higher  $M_n$  (19600 g.mol<sup>-1</sup>), while the polymerization was still performed with good control. Further increase of the temperature to 70 °C (entry 7, Table 1) resulted in an even higher monomer conversion (84 %), leading to a polymer with  $M_n = 21900$  and relatively low polydispersity index (PDI = 1.18) in less than 2 hours. In each case, a good control over the polymerization reaction was obtained, as evidenced by the linear behavior of the first order kinetic plot and the linear increase of  $M_n$  as a function of conversion, while the PDI remains low (see Figure 4).

#### Figure 4

After deprotection of the PEEA-S-S-PEEA by a heating step at 80 °C for 24 h, PAA-S-S-PAA with the desired S-S bond is obtained. Brush surfaces were prepared from PAA-S-S-PAA (entry 3, Table 1) (see experimental part for details). The presence of the PAA polymer onto the substrates was confirmed by X-ray photoelectron spectroscopy (XPS). The C1s XPS spectrum of a PAA-functionalized gold substrate is shown in Figure 5. The C1s spectrum exhibits two main components. The peak centered at 284.9 eV is attributed to aliphatic carbon atoms while the one appearing around 289 eV is characteristic for the carbon atom of the carboxylic acid groups.

#### Figure 5

The PAA-functionalized gold surfaces were characterized by atomic force microscopy (AFM) in water. The influence of the pH of the aqueous environment on the surface properties was investigated. The characterization was done in water at a relatively low pH (pH = 5) on one hand, and at a relatively high pH (pH = 9) on the other hand.

The topographic images and the corresponding height profiles that were obtained by AFM in water at different pH values show the typical features of a brush regime in its collapsed and swollen state, respectively (see Figure 6). The pKa of PAA lies at about pH = 6 [32]. At pH equal to 5, PAA is expected to be protonated to a large extent and thus the polymer chains exhibit a relatively small hydrodynamic volume because of intramolecular H-bonding [32]. At pH equal to 9, the PAA chains are deprotonated and show a higher hydrodynamic volume, which is referred to as the “swollen” state. The topographic images and the height profiles show these typical features of the polymer chains in their “collapsed” (pH = 5) and “swollen” state (pH = 9). The average peak-to-valley distance increases from 0.4 nm at pH = 5 to 1.7 nm at pH = 9.

**Figure 6**

**Figure 7**

The thickness of the PAA layer can be estimated from AFM in the force spectroscopy mode. Figure 7 shows typical approach profiles, obtained in water at two different pH's, between the AFM tip and the PAA layer grafted on a gold substrate. The observed profile at pH = 9 (exponentially increasing repulsive forces during the approach) is the typical signature of a polymer brush under compression in a good solvent [33]. The linear increase of forces close to the contact point observed at pH = 5 is characteristic of a more collapsed state [34]. The average thickness of the swollen ( $7 \pm 2$  nm) and collapsed film ( $3 \pm 1$  nm) was estimated by the onset of the repulsive forces detected in the approach profiles. These results show an average collapse of the layer, expressed as the ratio of collapsed to swollen thickness, of about 0.4. The good collapsing capacity of the brushes is an indication that the grafting density regime is moderately dense. Indeed, for a high grafting density regime, the difference between collapsed and swollen brush thickness would be smaller. A crude estimation of the grafting density can be obtained from the measured thickness in the swollen state using the scaling

concept based on the Alexander–de Gennes model [14, 33, 34]. The scaling theory predicts that the equilibrium thickness of a polymer brush in a good solvent ( $L_0$ ) varies linearly with the degree of polymerization ( $N$ ), according to

$$L_0 \approx Nl \left( \frac{l}{d} \right)^{2/3}$$

where  $l$  is the size of the statistical segments and  $d$  is the average distance between the grafting points. This gives a distance of 7 nm between the grafting points, and thus a grafting density of  $\sim 2$  chains per  $100 \text{ nm}^2$ . Although this density may seem low, we are in a moderately dense brush regime. The Flory radius of the chains on the surface, estimated from the scaling concepts [35] is about 7 nm. The diameter of the coils is thus larger than the distance between grafting points, indicating that we are indeed in the brush regime.

## CONCLUSION

In conclusion, we have demonstrated that the functionalization of a gold surface with a pre-synthesized poly(acrylic acid) containing a disulfide (S-S) bond is an efficient and facile route to obtain pH-responsive switchable gold surfaces. The influence of the pH was demonstrated by atomic force microscopy. The topographic images, the corresponding height profiles and the force profiles all evidence a large collapsing/swelling capacity: the results show an average collapse of the layer, expressed as the ratio of collapsed to swollen thickness, of about 0.4. This high efficiency of the responsive behavior is an important feature for potential applications exploiting a change in film thickness, roughness or mechanical properties.

## ACKNOWLEDGEMENT

The work was supported by the Belgian Science Policy (IUAP VI/27 and a BELSPO post-doc fellowship for G. Grancharov) and the FNRS (FRFC 2.4512.07). S. D-C. is a Research Associate of the FRS-FNRS. W.V.C. thanks the Fund for Scientific Research – Flanders (FWO) for a postdoctoral fellowship.

## REFERENCES

1. Tokarev I, Motornov M, Minko S. Molecular-engineered stimuli-responsive thin polymer film: a platform for the development of integrated multifunctional intelligent materials. *J. Mater Chem* 2009; 19: 6932-6948.
2. Braunecker WA, Matyjaszewski K. Controlled/living radical polymerization: Features, developments, and perspectives. *Prog Polym Sci* 2007;32:93-146.
3. Hadjichristidis N, Iatrou H, Pitsikalis M, Mays J. Macromolecular architectures by living and controlled/living polymerizations. *Prog Polym Sci* 2006;31(12):1068-1132.
4. Matyjaszewski K. Macromolecular engineering: From rational design through precise macromolecular synthesis and processing to targeted macroscopic material properties. *Prog Polym Sci* 2005;30(8-9):858-875.
5. Matyjaszewski K, Tsarevsky NV. Nanostructured functional materials prepared by ATRP. *Nature Chem* 2009;1:DOI 10.1038/NCHEM.1257.
6. Advincula RC, Brittain WJ, Caster KC, Ruhe J. *Polymer Brushes: Synthesis, Characterization, Applications*. Weinheim: Wiley-VCH, 2004.
7. Zhao B, Brittain WJ. Polymer brushes: surface-immobilized macromolecules. *Prog Polym Sci* 2000;25(5):677-710.
8. Edmondson S, Osborne VL, Huck WTS. Polymer brushes via surface-initiated polymerizations. *Chem Soc Rev* 2004;33(1):14-22.
9. Lowe AB, Sumerlin BS, Donovan MS, McCormick CL. Facile preparation of transition metal nanoparticles stabilized by well-defined (Co)polymers synthesized via aqueous reversible addition-fragmentation chain transfer polymerization. *J Am Chem Soc* 2002;124(39):11562-11563.
10. Sumerlin BS, Lowe AB, Stroud PA, Zhang P, Urban MW, McCormick CL. Modification of gold surfaces with water-soluble (co)polymers prepared via aqueous reversible addition-fragmentation chain transfer (RAFT) polymerization. *Langmuir* 2003;19(14):5559-5562.
11. Zhu MQ, Wang LQ, Exarhos GJ, Li ADQ. Thermosensitive gold nanoparticles. *J Am Chem Soc* 2004;126(9):2656-2657.
12. Shan J, Nuopponen M, Jiang H, Kauppinen E, Tenhu H. Preparation of poly(N-isopropylacrylamide)-monolayer-protected gold clusters: Synthesis methods, core size, and thickness of monolayer. *Macromolecules* 2003;36(12):4526-4533.
13. Roth PJ, Kessler D, Zentel R, Theato P. A method for obtaining defined end groups of polymethacrylates prepared by the RAFT process during aminolysis. *Macromolecules* 2008; 41: 8316-8319
14. Duwez AS, Guillet P, Colard C, Gohy JF, Fustin CA. Dithioesters and trithiocarbonates as anchoring groups for the "grafting-to" approach. *Macromolecules* 2006;39(8):2729-2731.

15. Fustin CA, Colard C, Filali M, Guillet P, Duwez AS, Meier MAR, Schubert US, Gohy JF. Tuning the hydrophilicity of gold nanoparticles templated in star block copolymers. *Langmuir* 2006;22(15):6690-6695.
16. Fustin CA, Duwez AS. Dithioesters and Trithiocarbonates Monolayers on Gold. *J Electron Spectrosc Relat Phenom* 2009;172:104-106.
17. Hoogenboom R, Schubert US, Van Camp W, Du Prez FE. RAFT polymerization of 1-ethoxyethyl acrylate: A novel route toward near-monodisperse poly(acrylic acid) and derived block copolymer structures. *Macromolecules* 2005;38(18):7653-7659.
18. Goto A, Fukuda T. Kinetics of living radical polymerization. *Prog Polym Sci* 2004;29(4):329-385.
19. Gao HF, Matyjaszewski K. Synthesis of functional polymers with controlled architecture by CRP of monomers in the presence of cross-linkers: From stars to gels. *Prog Polym Sci* 2009;34(4):317-350.
20. Bernaerts KV, Du Prez FE. Dual/heterofunctional initiators for the combination of mechanistically distinct polymerization techniques. *Prog Polym Sci* 2006;31(8):671-722.
21. Van Renterghem LM, Lammens M, Dervaux B, Viville P, Lazzaroni R, Du Prez FE. Design and use of organic nanoparticles prepared from star-shaped polymers with reactive end groups. *J Am Chem Soc* 2008;130(32):10802-10811.
22. Kim BS, Gao HF, Argun AA, Matyjaszewski K, Hammond PT. All-Star Polymer Multilayers as pH-Responsive Nanofilms. *Macromolecules* 2009;42(1):368-375.
23. Dong HC, Zhu MZ, Yoon JA, Gao HF, Jin RC, Matyjaszewski K. One-pot synthesis of robust core/shell gold nanoparticles. *J Am Chem Soc* 2008;130(39):12852-+.
24. Tsarevsky NV, Matyjaszewski K. Reversible redox cleavage/coupling of polystyrene with disulfide or thiol groups prepared by atom transfer radical polymerization. *Macromolecules* 2002;35(24):9009-9014.
25. Tsarevsky NV, Matyjaszewski K. Combining atom transfer radical polymerization and disulfide/thiol redox chemistry: A route to well-defined (bio)degradable polymeric materials. *Macromolecules* 2005;38(8):3087-3092.
26. Bernaerts KV, Willet N, Van Camp W, Jerome R, Du Prez FE. pH-Responsive diblock copolymers prepared by the dual initiator strategy. *Macromolecules* 2006;39(11):3760-3769.
27. Dervaux B, Van Camp W, Van Renterghem L, Du Prez FE. Synthesis of poly(isobornyl acrylate) containing copolymers by atom transfer radical polymerization. *J Polym Sci, Part A: Polym Chem* 2008;46:1649-1661.
28. Van Camp W, Du Prez FE, Bon SAF. Atom transfer radical polymerization of 1-ethoxyethyl (meth)acrylate: Facile route toward near-monodisperse poly((meth) acrylic acid). *Macromolecules* 2004;37(18):6673-6675.
29. Patten TE, Matyjaszewski K. Atom transfer radical polymerization and the synthesis of polymeric materials. *Adv Mater* 1998;10(12):901-+.
30. Van Camp W, Germonpre V, Mespouille L, Dubois P, Goethals EJ, Du Prez FE. New poly(acrylic acid) containing segmented copolymer structures by combination of "click" chemistry and atom transfer radical polymerization. *React Funct Polym* 2007;67:1168-1180.
31. Wouters D, Van Camp W, Dervaux B, Du Prez FE, Schubert US. Morphological transition during the thermal deprotection of poly(isobornyl acrylate)-b-poly(1-ethoxyethyl acrylate). *Soft Matter* 2007;3(12):1537-1541.
32. Laguecir A, Ulrich S, Labille J, Fatin-Rouge N, Stoll S, Buffle J. Size and pH effect on electrical and conformational behavior of poly(acrylic acid): Simulation and experiment. *Eur Polym J* 2006;42(5):1135-1144.
33. Taunton HJ, Toprakcioglu C, Fetters LJ, Klein J. Forces between surfaces bearing terminally anchored polymer chains in good solvents. *Nature* 1988;332(6166):712-714.

34. Cuenot S, Gabriel S, Jerome R, Jerome C, Fustin CA, Jonas AM, Duwez AS. First insights into electrografted polymers by AFM-based force spectroscopy. *Macromolecules* 2006;39(24):8428-8433.
35. Degennes PG. Polymers at an interface - a simplified view. *Adv Colloid Interface Sci* 1987;27(3-4):189-209.

**Figure 1. Synthetic strategy for the preparation of poly(acrylic acid) (PAA) with a disulfide functionality.**

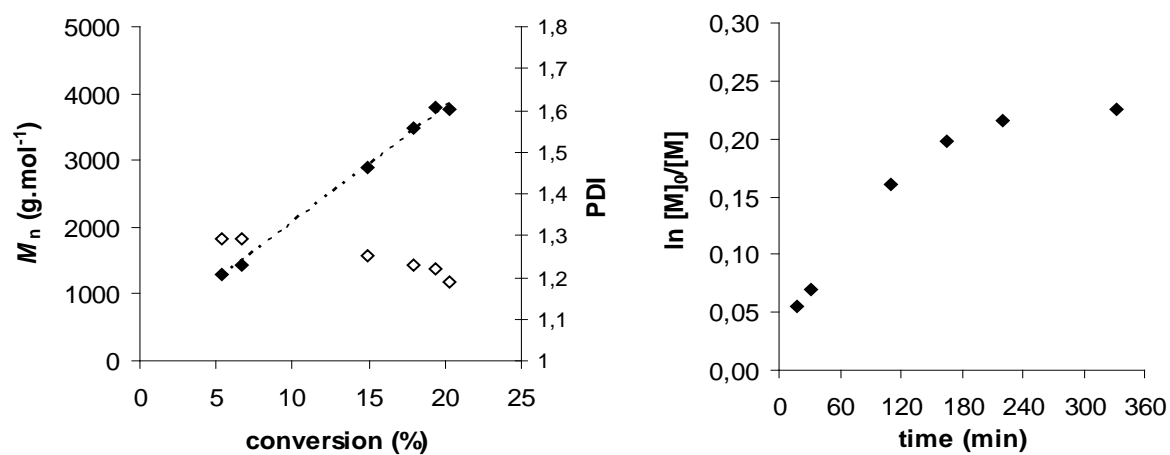


**Figure 2. Left: average molar mass ( $M_n$ ,  $\blacklozenge$ ) and polydispersity (PDI,  $\diamond$ ) vs. conversion (with trend line) for the polymerization of EEA using BHEDS(BP)<sub>2</sub> as initiator (Table 1, entry 1). Right: first order kinetic plot.**



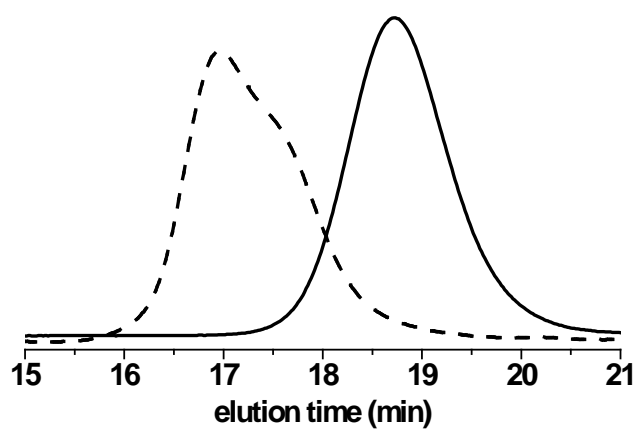


**Figure 3. GPC trace of the polymerization of EEA using a disulfide containing initiator BHEDS(BP)<sub>2</sub> (entry 1, Table 1– solid line; entry 2, Table 1 – dotted line).**

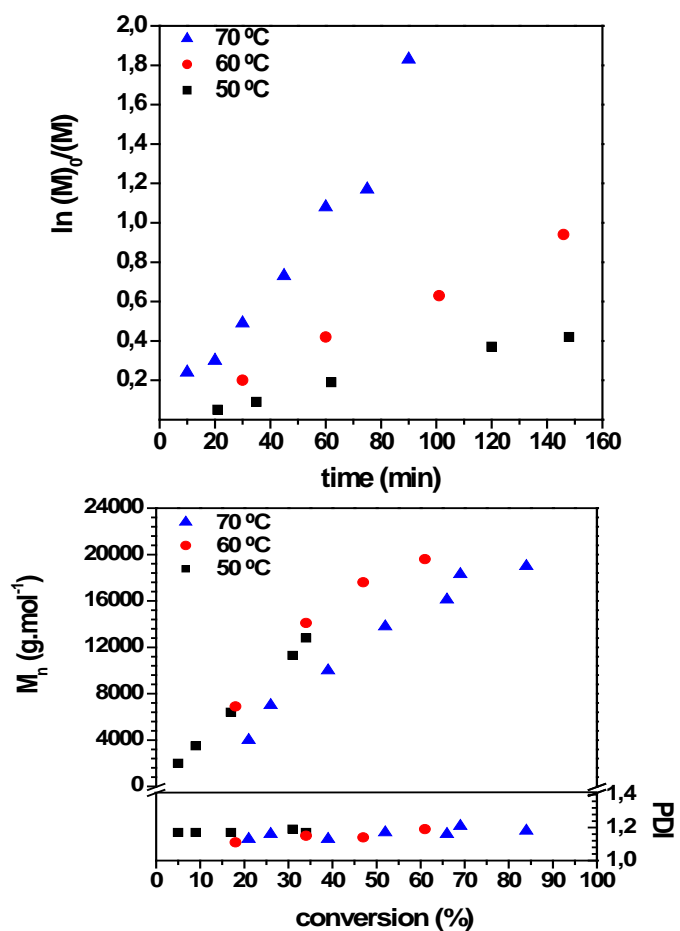


**Figure 4.** First order kinetic plot (top) and increase of  $M_n$  and evolution of PDI as a function of conversion (bottom) of the polymerization of EEA with disulfide containing initiator BHEDS(BP)<sub>2</sub> and ratio  $[M]_0/[In]_0/[Cu]_0/[ligand] = 200/1/2/2$  at 50, 60 and 70 °C (entry 3, 6 and 7 (Table 1), respectively).

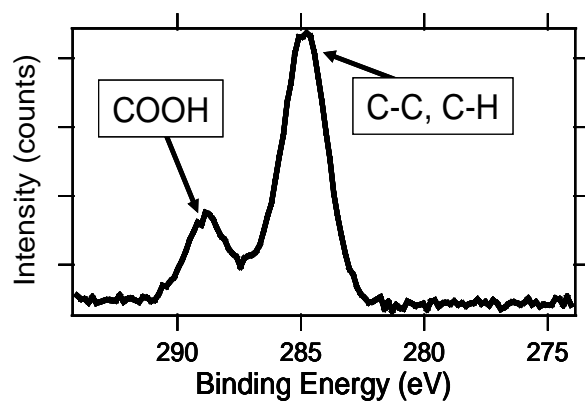


**Figure 5.** C1s XPS spectrum recorded on a gold substrate functionalized with PAA-S-S-PAA (entry 3, Table 1).

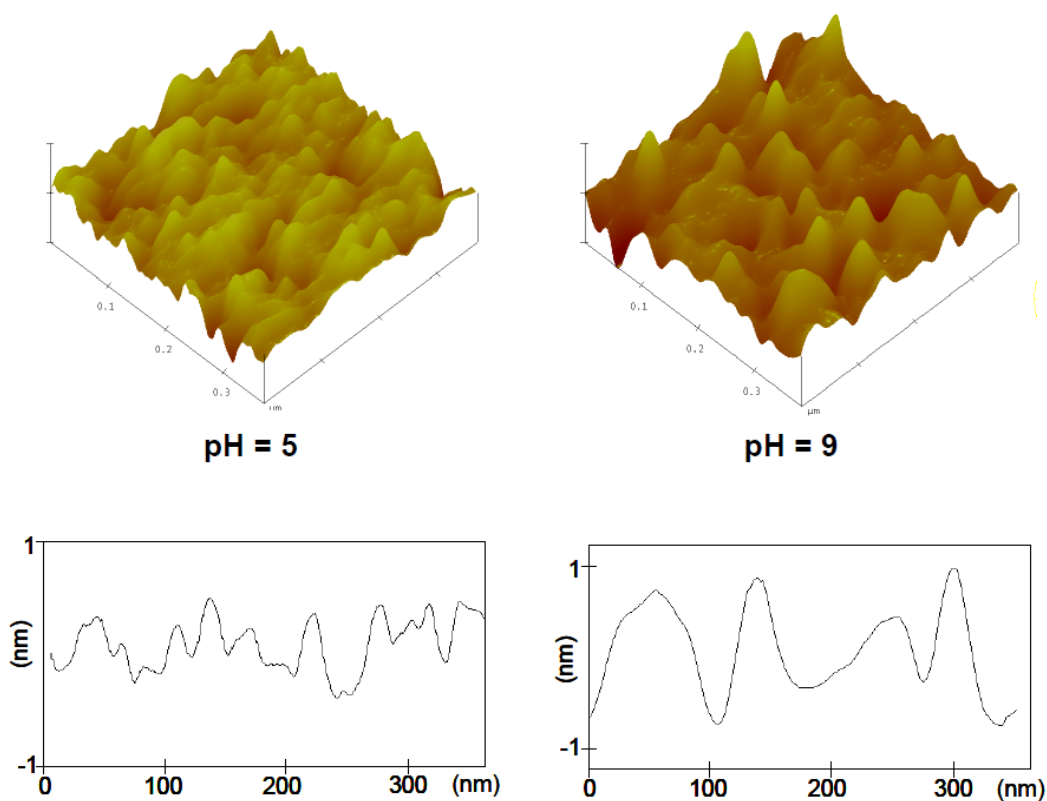


**Figure 6.** Topographic images (top,  $0.4 \times 0.4 \mu\text{m}^2$ , max z scale = 2 nm) and the corresponding height profiles (bottom) of a gold surface functionalized with PAA-S-S-PAA (entry 3, Table 1): collapsed state (at pH = 5) and swollen state (at pH = 9).

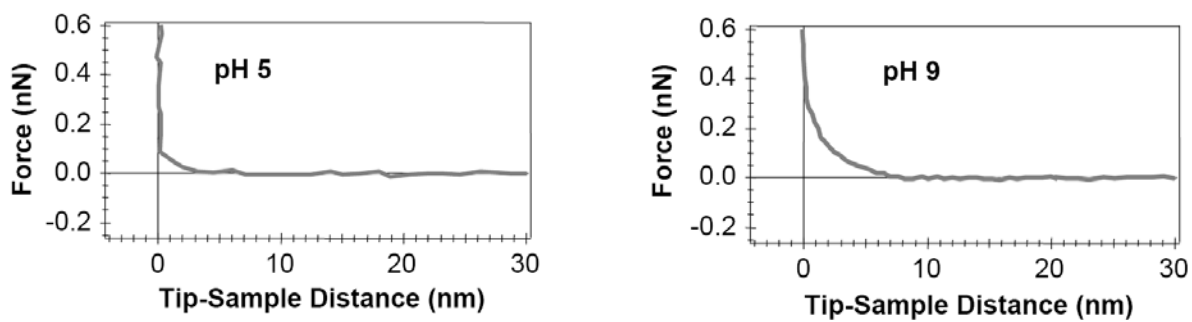


**Figure 7. Approach profile of a force curve obtained in water between an AFM tip and a gold surface functionalized with PAA-S-S-PAA (entry 3, Table 1) in the collapsed state (pH = 5, left) and in the swollen state (pH = 9, right).**

**Table 1. Summary of the reaction conditions and results of the polymerization of EEA by ATRP using BHEDS(BP)<sub>2</sub> as disulfide-containing initiator.**

Entry	[M] <sub>0</sub> /[In] <sub>0</sub> / [Cu] <sub>0</sub> /[ligand] <sup>a</sup>	Temp. (°C)	Time (min)	Conv. <sup>b</sup> (%)	M <sub>n,th</sub> (g.mol <sup>-1</sup> )	M <sub>n,exp</sub> <sup>c</sup> (g.mol <sup>-1</sup> )	M <sub>w</sub> /M <sub>n</sub> <sup>c</sup>
1	100/1/0.5/0.5	50	332	20	3300	3800	1.19
2	100/1/2/2	50	238	68	10200	12300	1.22
3	200/1/2/2	50	148	34	10200	12800	1.17
4	200/1/4/4	50	960	75	22000	23600	1.67
5	400/1/4/4	50	143	21	12500	12800	1.12
6	200/1/2/2	60	146	61	18000	19600	1.19
7	200/1/2/2	70	90	84	24600	21900	1.18

<sup>a</sup>. [M]<sub>0</sub>, [In]<sub>0</sub>, [Cu]<sub>0</sub> and [ligand] = initial concentration of monomer, initiator, copper catalyst and ligand respectively. <sup>b</sup>. Determined from <sup>1</sup>H NMR. <sup>c</sup>. GPC system calibrated versus polystyrene standards.

## GRAPHICAL ABSTRACT

### Poly(Acrylic Acid) with Disulfide Bond for the Elaboration of pH-Responsive Brush Surfaces

Wim Van Camp, Filip E. Du Prez\*, Halima Alem, Sophie Demoustier-Champagne\*, Nicolas Willet, Georgy Grancharov, Anne-Sophie Duwez\*

